JOURNAL OF MATERIALS SCIENCE 21 (1986) 3153–3161

The falling weight impact test applied to some glass-fibre reinforced nylons

Part 1 *Appraisal of the method*

A. E. JOHNSON
Pilkington Brothers plc, Research and Development Laboratories, Lathom, Ormskirk, Lancashire L40 5UF, UK

D. R. MOORE, R. S. PREDIGER
Research and Technology Department, Wilton, PO Box 90, Middlesborough, Cleveland TS6 8JE, UK

P. E. REED, S. TURNER
Department of Materials, Queen Mary College, Mile End Road, London E1 4NS, UK

Tests and experiments carried out in three laboratories on five glass-fibre reinforced nylon compounds have shown that relatively small differences in the electrical filtering lead to important differences in the observed response curves and to the interpretations placed on them. As a consequence, at a superficial level interlaboratory agreement is not good, but when the curves are properly interpreted in the light of supplementary information derived by techniques such as flash photography during the fracture process and low energy impact the agreement is much closer. The overall picture that emerges is that the method is reliable and informative, far more so than the uninstrumented method which now stands virtually discredited by the new evidence.

1. Introduction

In the 10 year period during which instrumented falling weight impact testing has developed from an innovation to an established evaluation technique there have been relatively few papers published on the subject; references [1–7] are typical of those that have been. In contrast to that public reticence, many data have been generated and many judgements concerning polymer and end-product development, fitness-for-purpose, quality, etc., have been made on the basis of those data. The explanation for the mismatch between published and unpublished results is quite innocent: the method is so informative and useful that its exploitation is more imperative than its validation through public scrutiny. However, public scrutiny offers a safeguard against the accidental adoption of unsound procedures, a route towards consensus and a starting point for standardization, and it is therefore an essential constituent of the infrastructure of technology. This paper makes a contribution to the validation process, though it was planned more as an exploration than with validation as a specific target. It presents results obtained in three independent laboratories on five glass-fibre reinforced nylons, some of which were novel compounds of commercial interest. The programme was genuinely collaborative in that the test specimens were taken from a common pool, the three test configurations all conformed to ISO/DIS6603/1, and adjustments to the three subprogrammes were made in the light of the shared and accumulating experience. On the other hand, it was not regimented, so the investigators were free to pursue whatever avenue seemed pertinent to their interests. The outcome has been three interconnected but individualistic studies with enough common ground to shed some light on the interlaboratory variability that is likely to arise with the method.

The common ground on which data from the three laboratories can be compared was a standard sized specimen, a disc 60 mm diameter, 2 mm thick impacted at 5 m sec^{-1}. However, as might be expected and as will become apparent, adherence to stipulations about specimen size and test geometry will not suffice alone to guarantee that the data are reliable or meaningful. In particular, noise in the primary data and the procedures by which they are processed can affect the final result quite markedly. For instance, noise can obscure important features or exaggerate unimportant ones and the data processing procedures can introduce further distortions. Since the three apparatuses differed in their facilities for signal detection and processing, some disparities arose, constituting a timely warning against over-facile interpretations of the data generated by instrumented apparatus. With such apparatus it is possible that correlations could be established between identifiable features on the response curve and stages in the development of damage in the specimen, but success in that hinges upon the ability to identify what is genuine material response and what is merely a consequence of extraneous vibrations. Flash photography of the tension face of the specimen at a preselected

0022–2461/86 $03.00 + .12

moment during the impact event has proved to be helpful in that context and, in conjunction with some low-energy impact tests, it has also provided interesting and important information on the onset of damage in the specimens.

Other experiments investigated the effect of variables such as impact velocity, specimen size and test configuration. Taken together, the results give a comprehensive picture of the impact resistance of some short-fibre reinforced nylons that could not have emerged from the limited resources of any one of the participating laboratories and would not have emerged had the programme been conceived as a regimented investigation of interlaboratory variability. However, since the investigation ranged widely and generated many data, it was deemed that a single paper would not have been a satisfactory vehicle for the dissemination of the results. Hence, this paper is the first of two; it is devoted mainly to a discussion of the techniques and the interpretation of typical data with no more reference to individual materials than is strictly necessary for the argument. The behaviour of the materials will be considered in the second paper.

2. Experimental details

Five different glass-fibre reinforced nylon compounds were used in the programme. Some of them are available commercially. others were specially formulated. The code by which they are referred to in this paper and certain pertinent details are set out in Table I.

The compounds were injection-moulded on a Demag D80 machine using the following conditions:

1st stage injection	=	20 bar
2nd stage injection	=	56 bar
Back pressure	=	10 bar
Melt temperature	=	280° C
Mould temperature	=	90° C
Screw speed	=	120 r.p.m.
Injection time	=	2.5 sec
Follow up time	=	8 sec
Cooling time	=	30 sec

The major proportion of each sample was moulded into edge-gated discs 60 mm diameter and about 2 mm thick. The mould had two nominally identical cavities but the mouldings have been distinguished by the letters "L" and "R". Thus specimens are identified where necessary in this paper and its sequel by a code number such as PA-1L/33 which gives the sample (PA-1), the cavity (L) and the shot number (33). Subsidiary batches of mouldings were edge-gated discs, 100 mm diameter, 3 mm thick and 50 mm diameter, 2 mm thick.

Each collaborating laboratory, designated P, Q and W in this paper, had its own falling weight impact machine; that in Laboratory Q was a CEAST Advanced Fractoscope System Mark 3 and those in the other two laboratories were home-made. A description of the one in Laboratory W has been published [2]. In the tests, the specimens were freely supported on an annulus of radius 20 mm. The impactor has a hemispherical tip of radius 10 mm and the incident energy was far in excess of that needed to break the specimens. Tests were conducted at room temperature, at impact velocities of 1, 3 and 5 m sec^{-1}. All specimens were stored "dry".

TABLE I Sample codes and material specifications

Code	Description
PA-1	Nylon 66 + nominally 0.5 wt fraction of short glass fibres.
PA-2	Nylon 66 + nominally 0.5 wt fraction of longer glass fibres than PA-1.
PA-3	As PA-2 but approximately 0.3 wt fraction.
PA-4	Nylon 66 + nominally 0.3 wt fraction of short glass fibres + pigment.
PA-5	Nylon 6 + nominally 0.3 wt fraction of short glass fibres.

Any sudden contact between two bodies initiates vibrations and stress waves in both. If the impacted body is highly viscoelastic or plastic in nature the vibrations tend to be heavily damped, but glass-fibre reinforced nylons would be more correctly classified as elastic and brittle so the signal derived from an impact test on one is distorted by extraneous vibrations. The amplitudes and frequencies of these extraneous vibrations depend on various factors, including the architecture of the testing machine and the degree of electrical filtering imposed on the initial signal both of which differ on the three machines. Thus, the interpretation of the results and the coordination of the data emanating from the three laboratories was far from straightforward, as indeed seems to be so for all impact tests involving nearly-brittle specimens. In such cases, subsidiary experiments aimed at the identification of critical stages in the fracture process can be very helpful and in this study two such subsidiary techniques were employued. These were photography of the specimen at various pre-selected instants during the impact event and low-energy impact tests in which the specimen was damaged but not destroyed.

Precise timing is a fundamental requirement in the use of photography to assign the sequence of events which occur during impact failure to features of the force against time graph. This was accomplished experimentally by using a twin channel transient recorder (Nicolet 3091) which captured the force values on the first channel in the usual manner, and simultaneously determined the time when the photograph was taken by means of a large area photodiode connected to the second channel. This enabled the start, intensity, and duration of the flash to be measured during each impact event. An electronic timing device was used to delay the flash by a pre-set interval. The delay circuit was connected to the first channel of the transient recorder so that the voltage rise from the force transducer triggered the pre-set delay. With this arrangement the time when the flash reached its maximum intensity could be determined with an accuracy equal to the time interval between successive points, which was 2 μsec for the fastest sweep time. By progressively increasing the pre-set time delay for successive impact tests a series of

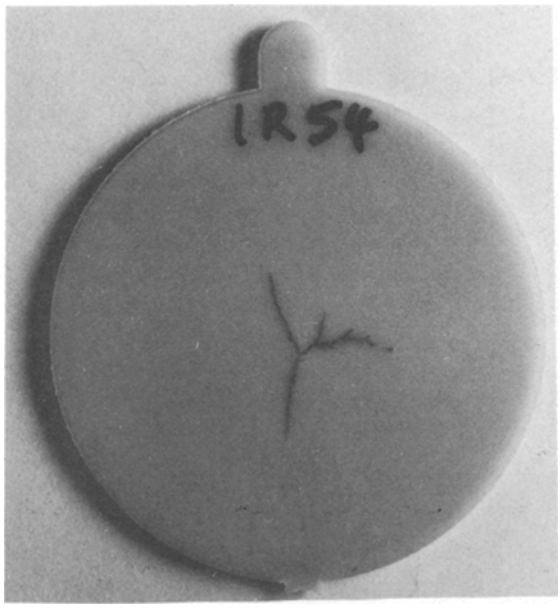

Figure 1 Typical damaged specimen for PA-3 after low-energy impact.

photographs was obtained covering each stage of the fracture process.

Low-energy impact tests were also developed and applied. The virtue of an impact test at an incident energy lower than that needed to break or rupture the specimen is that it may damage the specimen and capture a state through which it would have passed had the incident energy been overwhelming. In an excess energy test, on the other hand, the damage arising during the early stages of the impact event is often obscured by the subsequent damage. These glass-fibre reinforced nylons are particularly amenable to this approach because the fibres bridge the growing crack to some degree and thereby frustrate any tendency for the crack to propagate out of control, and by careful choice of incident energies successive stages of damage can be developed. Fig. 1 is a photograph of a typical damaged specimen. For all five grades, the damage almost invariably took the form of a three-branched crack initiating at the point of impact. The three main branches grew radially, with occasional and temporary deviations from the main direction. The crack lengths could always be measured approximately by means of a ruler and it transpired, as will be shown later, that for each grade there is a simple relationship between the incident impact energy and the total length of the generated crack. That information has a bearing on the interpretation of the force–time curves.

The apparatus used for the low-energy impacts (Laboratory Q) was not ideal for the task in that the low incident energies required could not be attained merely by reduction of the mass of the impactor and therefore the impact velocity was changed instead. With many materials it would be essential that energy and velocity were independently varied but in view of the nature of these particular materials and direct experimental evidence, it was deemed that the changed in impact velocity could be disregarded.

3. The response curve and its interpretation

3.1. The force–time curve–preamble

The force–time signal describing the impact event is dependent on material properties, electrical filtering and architecture of the apparatus. Laboratories P and W employed similar electronics except that the filters were 3.3 and 2.2 kHz, respectively; Laboratory Q had different electronics and the signal was not usually filtered. The architecture of the three testing machines differed, but examination of the qualitative features of the force–time signals from Laboratories P and W revealed them to be sufficiently similar to be taken as common.

Examples of force–time curves for sample PA-3 from an unfiltered source from Laboratory Q and the filtered source from Laboratory P/W are illustrated in Fig. 2. These are not "typical" of the material, because the individual curves for a set of specimens tested under nominally identical conditions vary greatly, for all three laboratories. In these situations, where the experimenter is faced with the difficulty of identifying characteristic features and physically significant features, the scope for error and misinterpretation is almost unlimited. In the curve from Laboratory Q for example, the first peak could be associated with the first crack, it could have arisen as the specimen settled on to the support ring under the initial contact with the impactor or it could be merely the first extraneous vibration on a force–time signal that would otherwise have increased monotonically from zero. Only in the first case would it have a physical significance. This

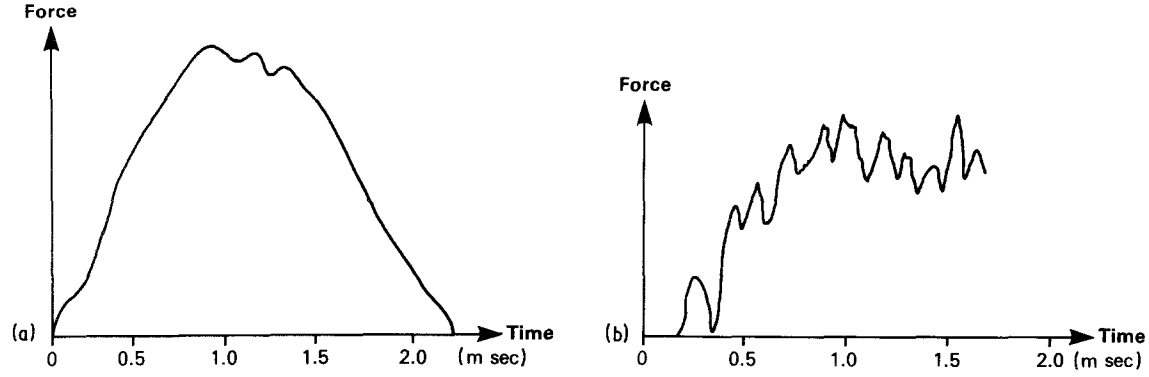

Figure 2 Force–time signals from sample PA-3. (a) Laboratory P/W, filtered signal, (b) Laboratory Q, unfiltered signal.

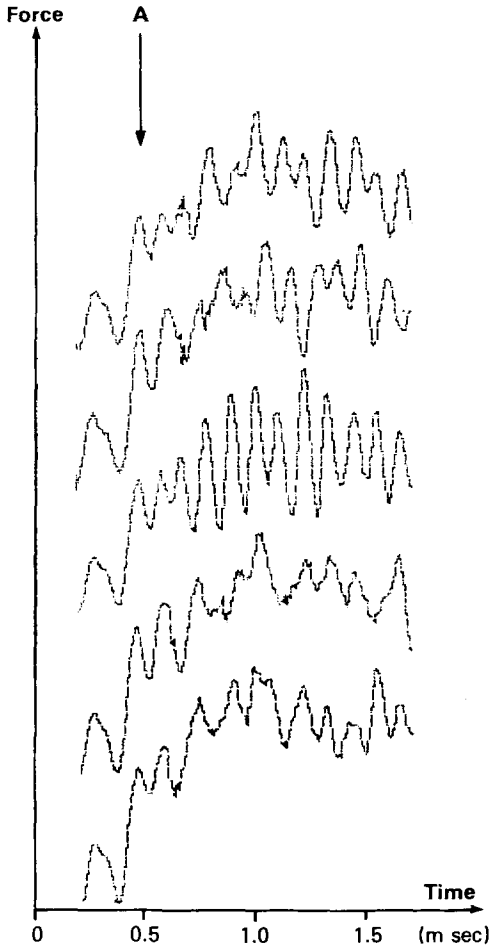

Figure 3 Force–time curves, unfiltered data. Compound PA-3, left-hand cavity.

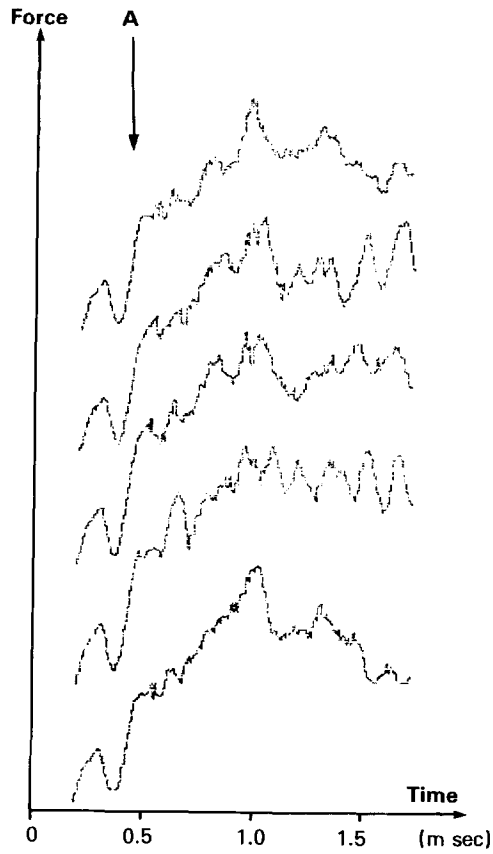

Figure 4 Force–time curves, filtered data. Compound PA-3, left-hand cavity, filter 9 kHz.

issue and many others are not easily resolvable, though some light is shed on the matter by three sets of experiments relating to filtering, photographic impact and low-energy tests.

3.2. Filter experiments

The testing machine in Laboratory Q was used to interpret the force–time curves in terms of the filter in the amplifier. Fig. 3 is the superposition of five unfiltered force–time curves where it can be seen that there is a common periodicity overall. After the first three cycles the coincidence between the successive peaks for the five specimens deteriorates, presumably as interference phenomena arise, but coincidence re-establishes itself from time to time thereafter and a frequency of about 9 kHz is evident. The same frequency has been noted in tests on other materials; it is thus a characteristic frequency of this particular apparatus. Accordingly, a narrow band 9 kHz filter was introduced for five more tests, the results from which are superposed in Fig. 4. The periodicity persists but, as one would expect, is much less dominant; the first peak also persists, though that too is affected.

The overall shape of the filtered curves suggests that the first peak is extraneous even though it survives the filtering. (This is further analysed in the next section.) The shape also suggests that the second peak in the unfiltered signals (labelled "A" in Fig. 3) may be significant. However, in the filtered curves that feature may reduce to a shoulder (also labelled "A", in Fig. 4) and, consequently, there may be some uncertainty in associating a failure mechanism with the feature.

It seems from Figs 3 and 4 that filtering is not unambiguously helpful; it distorts the apparent shape of the curve and possibly changes the magnitudes of the forces. However, under close scrutiny the magnitudes of the forces, deflections and energies that can be extracted from the recorded signal do not appear to have been affected strongly or systematically by the filtering. Some mean vales of the data, derived from Figs 3 and 4 are shown in Table II: the sets are small, the coefficients of variation are large and therefore most of the differences between filtered and unfiltered data are statistically insignificant. The one possible exception is for that peak which coincides with the maximum force, which seems to have been reduced by filtering, as might be expected from general reasoning. This might, however, merely arise from an inconsistency in associating or assuming a common failure feature with this peak. The energy would not be expected to show any marked effect due to filtering because oscillations along the ordinate axis would largely cancel out through the integration process.

The filtering experiments are limited but they indicate that the use of the filter does not of necessity alter the quantitative analysis, provided that resonance associated with the apparatus is removed from the signal. The filtered (9 kHz) curves of Fig. 4 are more closely related to the filtered curves (2.2 kHz) from Laboratories P and W. An over-riding problem still remains, however, in terms of interpreting the features and multi-peaks in the force–time curves from all of the laboratories.

TABLE II Mean values of force, deformation and energy to compare filtered and unfiltered data. Impact velocity 5 m sec^{-1}, temperature 15 to 17° C, Laboratory Q

Material/Specimen	Signal condition	No. of specimens	Feature A (see Figs 3 and 4)			Maximum force peak		
			Force (N)	Deflection (mm)	Energy (J)	Force (N)	Deflection (mm)	Energy (J)
PA-3, left-hand cavity	Filtered 9 kHz	5	428(42)	1.72(0.27)	0.34(0.10)	670(51)	–	1.3(0.2)
	Unfilterted	5	458(41)	1.20(0.05)	0.20(0.04)	786(110)	4.01(0.45)	1.6(0.3)
PA-1, left-hand cavity	Filtered 9 kHz	5	460(23)	1.31(0.10)	0.26(0.03)	710(55)	2.75(0.52)	1.05(0.28)
	Unfiltered	3	433(29)	1.02(0.17)	0.18(0.05)	817(126)	2.79(1.00)	1.02(0.50)
PA-1, right-hand cavity	Filtered 9 kHz	5	550(0)	1.18(0.05)	0.24(0.01)	750(61)	3.64(1.34)	1.4(0.7)
	Unfiltered	3	500(50)	0.97(0.20)	0.15(0)	750(50)	3.03(0.62)	1.1(0.4)

Standard deviations in parentheses.

3.3. Photographed impact

The purpose in presenting single photographs of the tension surface of a specimen during impact, is to help interpret the complex features in the force–time curve. A sequence of photographs on different specimens but of increasing "energy-absorbed" conditions for sample PA-3 are illustrated in Figs 5 to 10. The experiments were conducted on a testing machine from Laboratory W with the electronic equipment for Laboratory P.

The figures illustrate both the force–time signals and the tension surface of the specimen during impact. The vertical line through the force–time curve indicates when the photograph was taken. A glance through the six different curves for nominally similar specimens gives further evidence for the atypical nature of any single curve, although certain of the features are common.

A clearer interpretation of the first peak is now possible. Fig. 5 illustrates no failure on the tension surface of the specimen at a time just after the first peak. It is therefore evident that the first peak is not associated with the failure behaviour of the specimen. This peak is lost completely when thicker specimens of the same material are impacted, therefore it would appear to be stiffness related. A likely explanation of the origins of this first peak lie in the initial vibration established by a fast moving object striking a stationary specimen.

Fig. 9 illustrates the tension surface coincident in time with the next obvious peak in the force–time curve. A well established crack is seen. Interestingly, this peak in Fig. 9 is unlikely to be the feature A referred to in Fig. 3. Certainly, the timescale of events supports this view, but so, too, do the various changes of slope (as opposed to "peaks") prior to this point on the force–time curve. There is an implication here that the electronic smoothing of the curve has diluted the resolution in likely important areas of the response-curve. (It could also be argued that lack of filtering overcomplicates the response curve.)

Fig. 6 illustrates approximately that position on the force–time curve where a crack initiates. The crack that is just observable in this figure might only have initiated in the tension surface and might yet have to propagate through the thickness of the specimen. Further work is necessary in order to develop this point. The slope of the force–time curve does change at several points between the first peak and the next main peak. These changes in slope are associated with both initiation and propagation of the crack as illustrated in Figs 5 to 8.

The peak associated with maximum force is seldom the first significant feature on the response curve; furthermore, there is clear evidence from Figs 5 to 10 that for this sample of PA-3 the first crack initiates before the first significant feature arises, irrespective of how the latter is manifest.

3.4. Low-energy impact

Several of the samples are subjected to the low energy test. Fig. 11 illustrates the results for PA-3 in a graph of total crack length (on the tension surface) plotted against drop height/incident energy. The drop heights

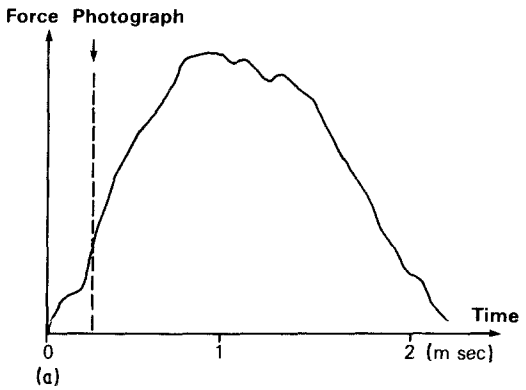

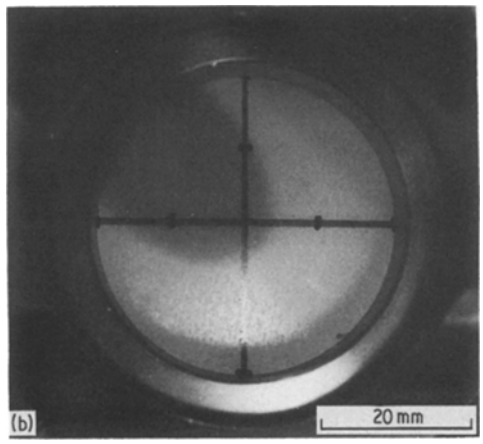

Figure 5 (a) Force–time curve, and (b) photograph taken at absorbed energy of 0.1 J. Material PA-3.

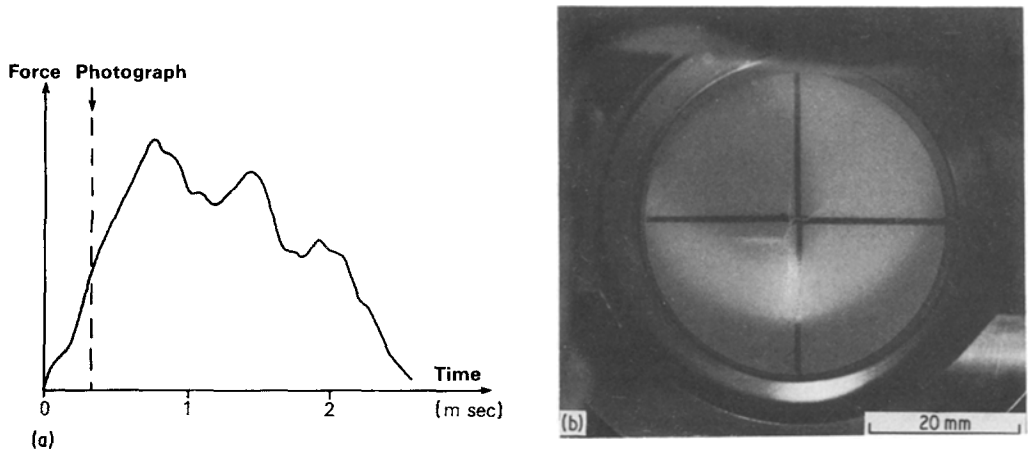

Figure 6 (a) Force–time curve, and (b) photograph taken at absorbed energy of 0.2 J. Material PA-3.

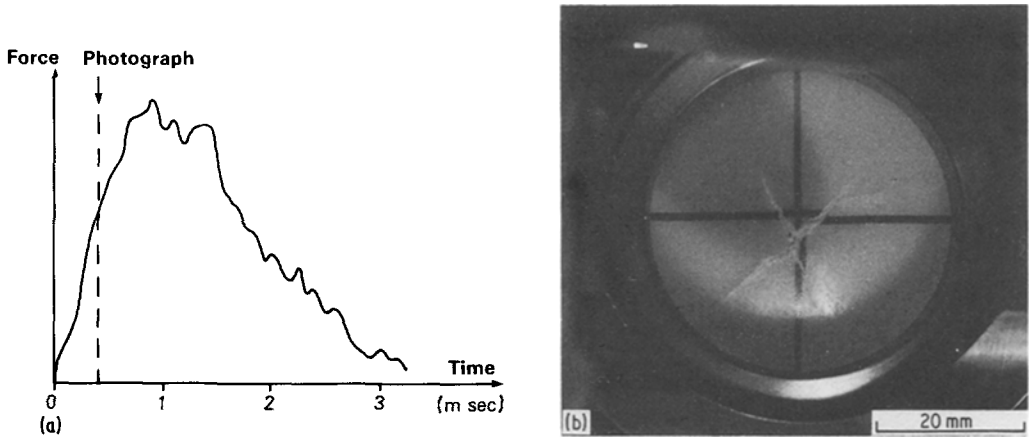

Figure 7 (a) Force–time curve, and (b) photograph taken at absorbed energy of 0.5 J. Material PA-3.

were small and the possible error near zero correspondingly large, but a conservative estimate suggests that the energy of 0.34 J listed in Table II as the energy to the first significant peak (feature A) would have generated at least 10 nm of crack. (Data for the other materials lead to similar estimates.)

This can be compared with the observation in Fig. 7 where 0.38 J energy has been applied at the point of triggering the flash-gun to initiate the photography. About 25 mm of crack has been established. The exact crack dimensions and close agreement between the two cases could not be expected because the tests were conducted at different speeds. The important conclusion is that the first significant peak of the filtered curves from Laboratories P and W is not the same as Feature A of the curves from Laboratory Q; in all these cases the specimens had already cracked. It is possible, however, that for the features A of Table II, that the surface crack has only just developed through the thickness of the specimen, although only further experimental work can substantiate such a speculation.

4. Inter-laboratory comparisons

Comparisons between the data generated in the three laboratories are conducted for an impact velocity of

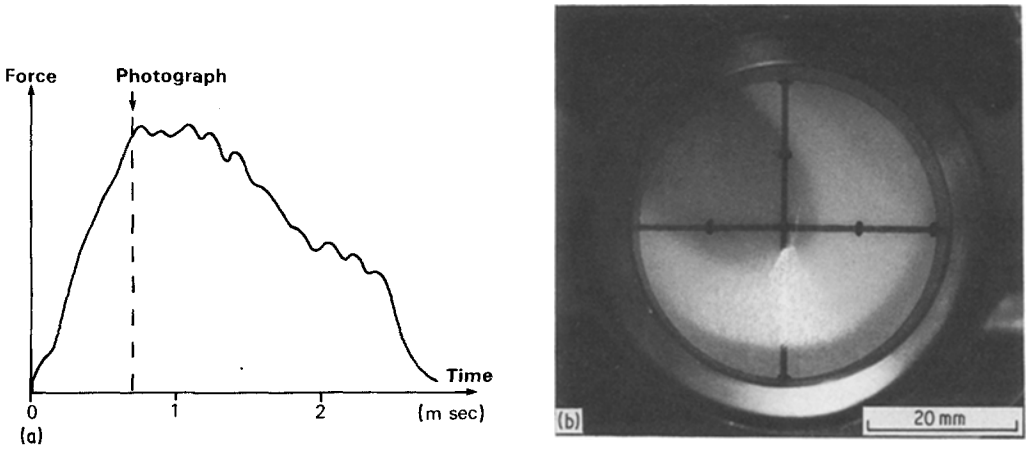

Figure 8 (a) Force–time curve, and (b) photograph taken at absorbed energy of 1.2 J. Material PA-3.

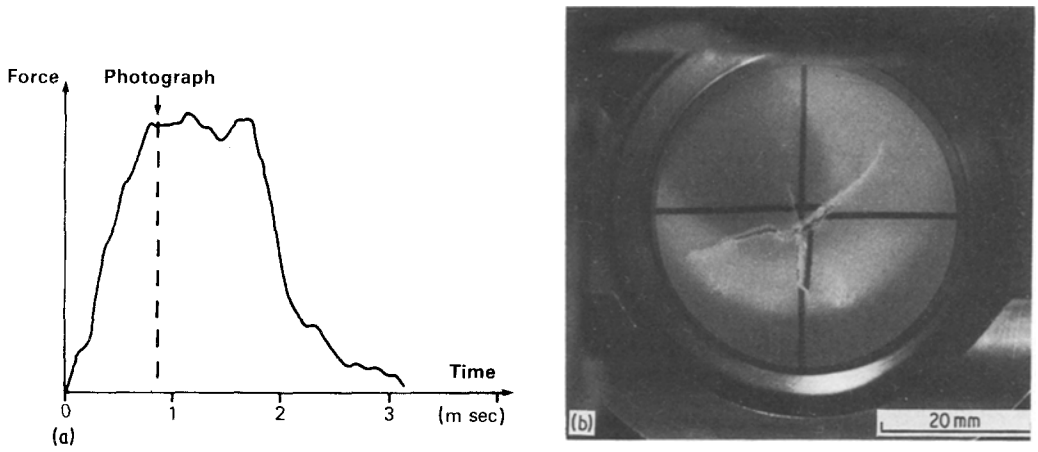

Figure 9 (a) Force–time curve, and (b) photograph taken at absorbed energy of 1.7 J. Material PA-3.

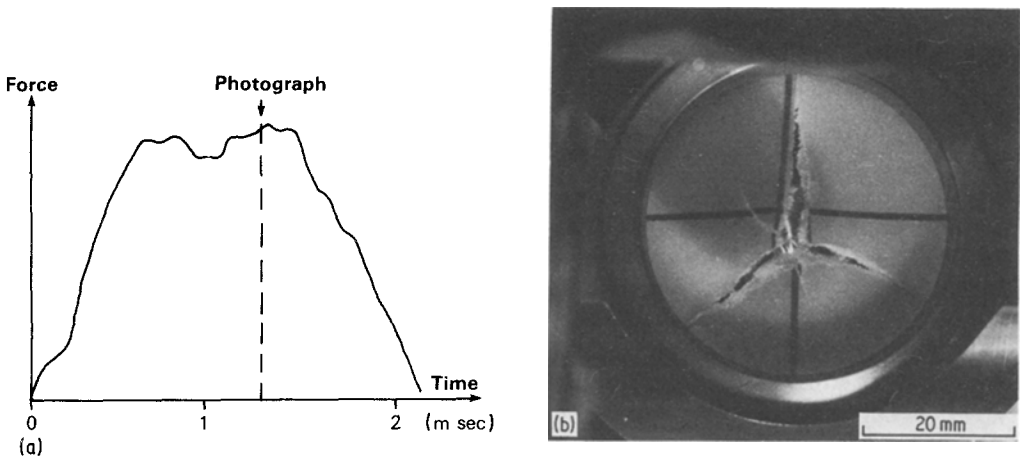

Figure 10 (a) Force–time curve, and (b) photograph taken at absorbed energy of 2.0 J. Material PA-3.

5 m sec^{-1}. The results shed some light on the interlinked issues of interlaboratory variability and the interpretation of the force–time records. The test temperatures were about 20° C, fine control not being necessary for this class of material. There were usually ten specimens in each set, five matched pairs from the left-hand and right-hand cavities; the impact properties from the two cavities differ, probably just because the thicknesses differ, but the data have been merged from the purpose of the comparisons.

In Table III the mean value and standard deviations of the force, deflection and energy associated with the first signifcant peak are tabulated (for the laboratory Q data, feature A is taken as the first significant peak). The data from Laboratory Q are distinctly different from those from the other laboratories, so much so as

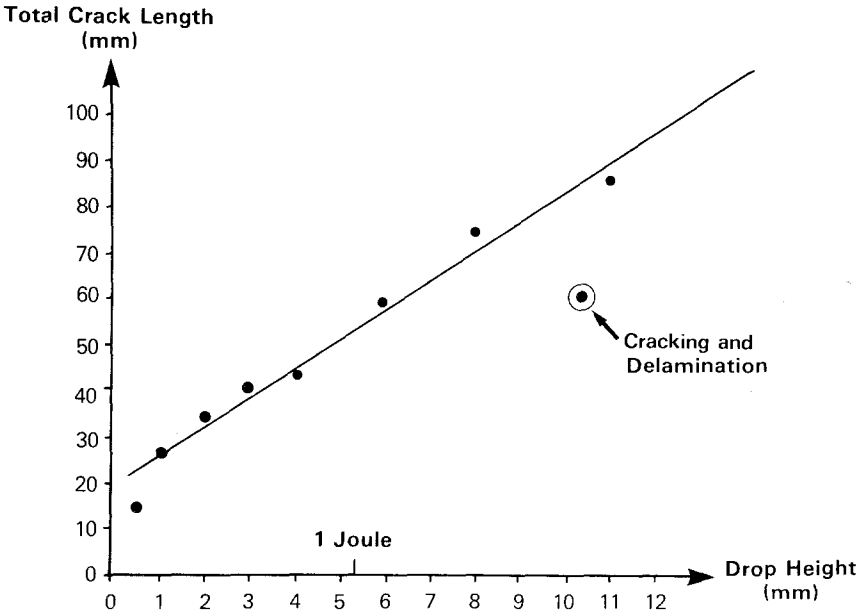

Figure 11 Damage by low-energy impacts. Compound PA-3 (30% wt/wt long fibres), left-hand cavity.

TABLE III Comparative data relating to the first significant peak. Impact velocity 5 m sec^{-1}

Material	Laboratory	Peak force (N)	Deflection (mm)	Energy (J)
PA-1	P	648(100)	2.6(0.8)	0.9(0.5)
	Q	467(52)	1.0(0.1)	0.17(0.03)
	W	666(41)	2.5(0.6)	0.8(0.4)
PA-2	P	977(44)	4.1(0.2)	2.1(0.1)
	W	878(74)	4.1(0.3)	1.9(1.3)
PA-3	P	739(111)	3.9(0.6	1.6(0.4)
	Q	486(53)	1.3(0.8)	0.2(0.03)
	W	709(55)	4.5(0.6)	1.8(0.4)
PA-4	P	576(27)	2.7(0.6)	0.8(0.9)
	W	697(57)	2.7(0.1)	0.7(0.1)
PA-5	P	496(33)	2.8(0.6)	0.7(0.3)
	W	591(50)	2.7(0.1)	0.6(0.1)

Standard deviations in parentheses.

to support the discussions raised in the previous sections as to its physical significance.

In Table IV the comparison between the data in Table III for Laboratories P and W is expressed as a set of ratios. From that it would seem that there is agreement, within the limits set by experimental error, between the laboratories. In order to involve Laboratory Q in a comparison it is necessary to use data at a peak corresponding to maximum force. Unfortunately, Laboratory W do not incorporate this into their analytical software, consequently only Laboratories Q and P can be involved. Table V shows no statistically significant differences between the data for the two laboratories, the standard deviations being very large, though the peak forces from Laboratory Q are consistently higher than those from Laboratory P, which may reflect the absence of filtering on the former.

Another comparison is of the data relating to notional final fracture, the deflections and energies for which are given in Table VI. This involves all three laboratories. The associated ratios are in Table VII. The energy ratios seem to be distributed randomly about unity but there is a bias about the deflection ratios, though the probability that six of the latter could be greater than unity just by chance is 0.062, and hence the apparent bias is only moderately significant in a statistical sense. However, interesting though these considerations are, there is little to be gained by pursuing them here because at final fracture the

TABLE IV Data from Table III expressed as ratios. Laboratories P and W

Material	Values from Laboratory W as a fraction relative to values from Laboratory P		
	Force	Deflection	Energy
PA-1	1.03	0.96	0.89
PA-2	0.90	1.00	0.90
PA-3	0.96	1.15	1.13
PA-4	1.21	1.00	0.87
PA-5	1.19	0.96	0.86
Average	1.06(0.14)	1.01(0.08)	0.93(0.11)

Standard deviations in parentheses.

TABLE V Comparative data relating to the maximum force. Impact velocity 5 m sec^{-1}

Material	Laboratory	Peak force (N)	Deflection (mm)	Energy (J)
PA-1	P	711(64)	3.9(0.2)	1.7(0.2)
	Q	783(93)	2.9(0.8)	1.1(0.4)
PA-3	P	772(61)	4.5(0.5)	1.9(0.4)
	Q	829(101)	4.3(0.6)	1.8(0.5)

Standard deviations in parentheses.

impactor still experiences a force. Photographic evidence is shown in Fig. 12. Therefore, the usual practice of registering zero force as final fracture must be misleading. In uninstrumented tests this error cannot be avoided.

5. Concluding comments in relation to inter-laboratory comparisons

In summarizing the inter-laboratory comparisons for these fibre-reinforced composites, it is clear that a superficial comparison would have revealed poor agreement. The supporting experimental studies have explained most of the reasons for this. First, it is important that the criteria for comparisons between different force–time curves relate to the same stages of the fracture process and not merely to some superficial similarity in the appearance of the curves. It is likely that electronic filtering can frustrate a comparison because a filter can transform a peak into a minor change of slope. The filter does not seem to affect the force measurement at that event to any significant degree. Second, a comparison of crack initiation is difficult unless supplementary evidence is available to identify the time at crack initiation. None of the laboratories indexed this event as a peak in the force–time curve, and there remains a need to define the initiation process and to resolve differences between cracks in the tension surface and through thickness cracks.

The energies to total fracture as measured in the three laboratories agree reasonably well. Unfortunately, there is strong evidence to indicate that

TABLE VI Comparative data relating to final fracture. Impact velocity 5 m sec^{-1}

Material	Laboratory	Deflection (mm)	Energy (J)
PA-1	P	9.6(0.8)	4.0(0.6)
	Q	9.2(1.2)	3.5(0.5)
	W	10.4(1.1)	4.1(0.4)
PA-2	P	11.7(2.2)	6.0(0.7)
	W	16.8(4.9)	7.2(0.7)
PA-3	P	11.3(1.5)	4.8(0.5)
	Q	13.9(2.3)	5.1(0.8)
	W	14.5(5.2)	5.5(1.1)
PA-4	P	10.0(0.5)	3.8(0.4)
	W	11.4(0.9)	3.7(0.2)
PA-5	P	9.5(0.8)	3.8(0.2)
	W	13.1(1.6)	3.5(0.3)

Standard deviations in parentheses.

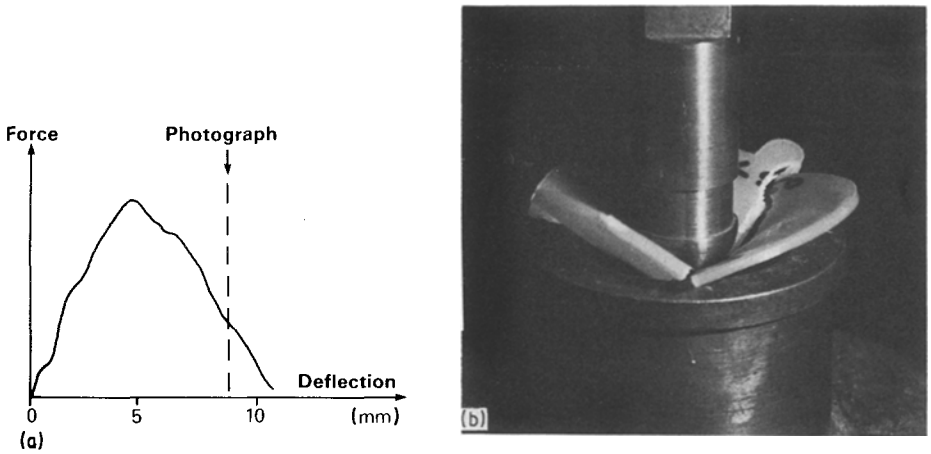

Figure 12 (a) Force–deflection curve. (b) Photographed impact near apparent final fracture, viewed from impacted (top) surface.

geometric factors as opposed to mere material factors provide large energy contributions to this measurement. This diminishes the value of this parameter in instrumented tests unless the instant of failure is identified, and it certainly discredits uninstrumented impact tests.

This is the first occasion that three laboratories have attempted to link their IFWI tests in such a detailed manner. What emerges comprises a list of difficulties much of which can be accommodated and accounted by further supportive work. The nature of the materials also complicated the comparisons. The fact that much could be resolved between the three laboratories must be a good omen for the future success of an informative impact technique, but the difficulties of interpretation of the force–time curves for composites can only be ignored at peril. It follows, also, that simple inter-laboratory comparisons of the type likely in "round-robin" exercises will generally yield results implying poor agreement.

TABLE VII Data from Table VI expressed as ratios

Material	Laboratory	Values from Laboratories Q and W as a fraction relative to values from Laboratory P	
		Deflection	Energy
PA-1	Q	0.96	0.87
	W	1.08	1.03
PA-2	W	1.44	1.20
PA-3	Q	1.23	1.06
	W	1.28	1.15
PA-4	W	1.14	0.81
PA-5	W	1.38	0.92
Average		1.21(0.17)	1.01(0.15)

Standard deviations in parentheses.

Acknowledgements

Two of the authors (PER and ST) gratefully acknowledge the financial support of the Polymer Engineering Directorate.

References

1. J. J. MOOIJ, *Polymer Testing* **2** (1981) 69.
2. P. A. GUTTERIDGE, C. J. HOOLEY, D. R. MOORE, S. TURNER and M. J. WILLIAMS, *Kunststoffe German Plastics* **72**(9) (1982) 10.
3. T. CASIRAGHI, G. CASTIGLIONI and G. AJROLDI, *Plastis Rubber Proc. Applic.* **2**(4) (1982) 353.
4. P. ZOLLER, *Polymer Testing* **3** (1983) 197.
5. S. TURNER, P. E. REED and M. MONEY, *Plastics Rubber Proc. Applic.* **4**(4) (1984) 369.
6. T. G. MEIJERING, *ibid* **5**(2) (1985) 165.
7. D. P. JONES, D. C. LEACH and D. R. MOORE, *ibid.* **6**(1) (1986) 67.

Received 23 August
and accepted 23 October 1985